

N O T I C E

THIS DOCUMENT HAS BEEN REPRODUCED FROM
MICROFICHE. ALTHOUGH IT IS RECOGNIZED THAT
CERTAIN PORTIONS ARE ILLEGIBLE, IT IS BEING RELEASED
IN THE INTEREST OF MAKING AVAILABLE AS MUCH
INFORMATION AS POSSIBLE



Technical Memorandum 80557

Examination of Lambertian and Non-Lambertian Models for Simulating the Topographic Effect on Remotely Sensed Data

Chris Justice and Brent Holben

(NASA-TM-80557) EXAMINATION OF LAMBERTIAN
AND NON-LAMBERTIAN MODELS FOR SIMULATING THE
TOPOGRAPHIC EFFECT ON REMOTELY SENSED DATA
(NASA) 25 p HC A02/MF A01

CSSL 05B

N80-12533

Unclas

G3/43 41473

SEPTEMBER 1979

National Aeronautics and
Space Administration

Goddard Space Flight Center
Greenbelt, Maryland 20771

EXAMINATION OF LAMBERTIAN AND NON-LAMBERTIAN
MODELS FOR SIMULATING THE TOPOGRAPHIC EFFECT ON
REMOTELY SENSED DATA

Chris Justice*
Brent Holben
Earth Resources Branch, Code 923

*Chris Justice is a National Research Council Resident Research Associate.

NASA/GODDARD SPACE FLIGHT CENTER
Greenbelt, MD 20771

EXAMINATION OF LAMBERTIAN AND NON-LAMBERTIAN
MODELS FOR SIMULATING THE TOPOGRAPHIC EFFECT ON
REMOTELY SENSED DATA

Chris Justice
Brent Holben

ABSTRACT

The differential illumination of surfaces due to slope angle and aspect variations produces a phenomenon known as the "topographic effect." This effect complicates the task of multispectral cover classification using remotely sensed satellite data of mountainous terrain. As a preliminary step to developing a technique to eliminate the topographic effect from remotely sensed data, two radiance simulation models were examined and compared. A Lambertian and a non-Lambertian model were tested using hand-held radiometer measurements from a uniform surface at different slope angle aspect orientations. A two-band, hand-held radiometer, filtered for the red and photographic infrared portion of the spectrum, was used to measure the radiance from a uniform sand surface over a range of solar elevations.

Linear correlation coefficients for the non-Lambertian model and the field spectra were calculated to be greater than 0.92 for all cases; whereas correlation coefficients for the Lambertian model ranged from 0.06 to 0.98. An assumption regarding an empirical constant within the non-Lambertian equation was found to be invalid and the model was improved by using subsets of the data to derive the empirical value.

CONTENTS

	<u>Page</u>
A. Introduction	1
B. Lambertian and Non-Lambertian Models	2
C. Data Analysis & Results	4
Summary of Results	7
Potential Application of the Models to Remotely Sensed Data	8
Bibliography	9
Acknowledgments	10

EXAMINATION OF LAMBERTIAN AND NON-LAMBERTIAN MODELS FOR SIMULATING THE TOPOGRAPHIC EFFECT ON REMOTELY SENSED DATA

A. Introduction

Several researchers have shown that the effect of topographic variation over a remotely sensed image can greatly complicate the task of multispectral classification of surface cover types (Cicone et al, 1977; Hoffer and Staff, 1975; Justice, 1978). The topographic effect is caused by differential illumination of ground surfaces due to slope angle and aspect variations and results in surface cover types having a wide range in radiance values (Sadowski and Malila, 1977; Holben and Justice, 1979). There is a need to eliminate the topographic effect prior to classification or to include consideration of the topographic variation within the analysis to improve Landsat multispectral classification accuracies in areas of rugged terrain (Strahler et al, 1978).

As a preliminary step to developing a technique to normalize remotely sensed data for topographic effects, Holben and Justice (1979) tested the suitability of a theoretical Lambertian model to simulate the topographic effect. The authors collected hand-held radiometric data of a uniform sand surface oriented at a complete range of slope angles and aspects for several solar elevations and correlated the radiance measurements to a simple Lambertian model. The results of this study showed that the Lambertian assumption was valid for certain cases and that Landsat data should be stratified according to surface incidence angle to provide improved cover classification. In a recent paper, Smith et al (1979) adopted a different approach and examined Landsat radiance data for coniferous forest sites with different slopes and aspects in Colorado for one solar elevation. A non-Lambertian model proposed by Minnaert (1941) was adopted and correlated to the Landsat data. The authors concluded that the Lambertian assumption was only applicable to a limited range of slopes and aspects of natural surfaces and that the non-Lambertian model provided an improved correlation.

Problems in ground location, site uniformity, the range of slopes, aspects and dates of imagery available, make radiance model testing using Landsat data a difficult task. To avoid these problems

and reduce some of the variables likely to affect the testing of the radiance models, a ground measurement procedure was adopted. The non-Lambertian model used by Smith et al (1979) was applied to the hand-held radiometric data sets collected by Holben and Justice (1979). Although only relevant for one cover type, the radiometer data represents a controlled set of radiance measurements for a complete range of slope aspects and solar elevations, thereby providing a suitable test set for the radiance model.

B. Lambertian and Non-Lambertian Models

Before examining the statistical relationships between the radiance models to the field measured spectral data, it is necessary to describe the Lambertian and non-Lambertian models. The geometric relationships between the sun, sensor and ground surface used in the description of the models are shown in Figure 1. The critical angles in the formulation of the models are the incidence and exitance angles. The incidence angle (i) is the angle formed between the sun and the surface normal. The exitance angle (e) is formed between the sensor and the surface normal. Simplistically, the radiance received by a sensor can be viewed as a function of the amount of light falling on the surface, the scattering properties of the surface and scattering properties of the medium between the sensor and the surface. The light falling on the ground surface can be described in terms of direct and diffuse irradiance. The direct irradiance is the parallel light radiating directly from the sun. The diffuse light is multidirectional and is composed of light scattered onto the surface by the atmosphere or surrounding ground surfaces. Under clear sky, non-hazy conditions, the diffuse component is a small proportion of the total irradiance, e.g., 12% of the total (Smith et al, 1979). Neither of the radiance models consider the diffuse light component and the implications of this omission are discussed below. The scattering properties of the surface are a function of the surface composition and roughness and are difficult to model. Two special cases of scattering, however, are relatively easy to model for direct irradiance and provide reference points within a wide range of possibilities. A completely specular surface is one from which the radiance is monodirectional in the angle of reflectance, e.g., a mirror. The second special case is the Lambertian surface which scatters light equally in all directions

and therefore can be modelled simply as a function of the cosine of the incidence angle (Monteith, 1962). It is clear that most natural surfaces are non-Lambertian having preferred directions of scattering (Kriebel, 1978). Radiance from a non-Lambertian surface, therefore, must be modelled by considering both incidence and the directional scattering from the surface. Smith et al (1979) proposed an empirical model which included incidence and exitance as a function of an empirical constant, "K," which indicates the "Lambertianess" of the surface. The non-Lambertian model is shown in Equation 1:

$$L = L_n (\cos^k i * \cos^{k-1} e) \quad (1)$$

Where: L = Radiance

L_n = Radiance when $i = e = 0$

i = Incidence

e = Exitance

K = Minnaert Constant

The empirical constant "K" was developed by Minnaert (1941) and was used for photometric analysis of lunar surfaces. The "K" value is derived by linearizing the equation.

$$\log(L * \cos e) = \log L_n + K * \log (\cos i * \cos e) \quad (2)$$

If $\log(L * \cos e)$ is plotted against $\log (\cos i * \cos e)$ then "K" is the slope of the regression line. A Lambertian surface would have a "K" value equal to 1 (Minnaert, 1961). Minnaert (1941) stated that "K" represented the roughness of the surface and varied as a function of phase angle (i.e., the angle between the sensor and the light source). Sytinskaya (1949) examined the Minnaert photometric function more closely for several surface types and showed how most natural surfaces had "K" values of less than unity. Vegetated surfaces were shown to have small or negative values of "K" and mirror-like materials with a high specular component such as opal and glass, had values exceeding unity.

Smith et al (1979) applied the Minnaert function to their slope and aspect data and calculated "K" values for *Pinus ponderosa* of between 0.26 and 0.37 for the four multispectral channels. "K" was shown to vary as a function of wavelength.

C. Data Analysis & Results

The objective of the analysis was to correlate the non-Lambertian radiance model proposed by Smith et al (1979) with field measured radiances and to compare the results with those obtained using the Lambertian model tested by Holben and Justice (1979). The same data set used by Holben and Justice (1979) was applied to the non-Lambertian model. The data set consisted of hand-held radiometer measurements taken of a uniform sand surface at four different solar elevations. The measurements, taken at a range of slope angles and aspects, are described in detail by Holben and Justice (1979).

Before correlating the non-Lambertian model with the field data, it was necessary to calculate the photometric constant "K" for each of the four data sets by linearizing the equation, as shown in Equation 2.

Table 1 shows the "K" values calculated for each of the four data sets using all of the data. The "K" values varied from .663 to .504 with phase angles from 29° – 76°. These results are consistent with those presented by Stytsinskaya (1949) who obtained a "K" value of 0.53 for dry sand and Minnaert (1941) who stated that K varied as a function of phase angle. Although a general decrease in "K" value with decreasing phase angle can be seen from the present results, this relationship is by no means conclusive.

Smith et al (1979) described "K" as a constant but demonstrated that by calculating "K" using a subset of this slope and aspect data, a different value was obtained than when using all the data. This led us to examine whether "K" varied as a function of aspect and slope. Aspect is the aspect of a slope relative to the sun's azimuth (Holben and Justice, 1979). First, "K" values were calculated for each aspect of the four data sets and are presented in Table 2. For each of the data sets, "K" was found to vary substantially with aspect generally decreasing away from solar azimuth. The greatest range in "K" values was found for the 40° solar elevation data set, where "K" had a range of 0.370. The "K" values for each of the data sets have a sinusoidal shape (Figure 2) with the lowest "K" values appearing at the highest aspect angles. The smallest range of "K's" occurred for the highest solar elevation data set. Second, "K" values were calculated for each slope stratum within

each data set (Table 3). "K" was found to vary with slope for each data set with the greatest range in "K" values occurring for the 40° solar elevation data set. These results show that "K" varies significantly with slope and aspect and cannot be assumed to be constant for a given surface type regardless of the surface geometry.

The next step was to examine how the non-Lambertian model correlated with the field spectra and to compare the results with those obtained from the Lambertian model. To calculate the statistical correlation between the non-Lambertian model and the field data, Pearson's product moment correlation was used. The resulting correlation coefficients (r) values are presented in Table 4. Correlations were marginally higher for the non-Lambertian model than for the Lambertian model ($\cos i$) using all data points. Higher r values were obtained when the "K" values for each aspect were used within the non-Lambertian model. Comparison of the r values for the non-Lambertian model and the Lambertian model for each aspect (Table 4) showed that the non-Lambertian model was more highly correlated to the field radiance at higher solar elevations.

When using a subset of their data to show that the Lambertian assumption was satisfied for certain slopes and incidence angles, Smith et al (1979) derived a "K" value for Landsat Channel 5 of $.6 \pm .5$. On the basis of these results, we examined the sensitivity of the non-Lambertian model to variations in the "K" value, to see how correlations with the field spectra varied as a function of "K". A sensitivity test was designed to examine the correlation coefficients between the field measured radiance and the non-Lambertian model where the "K" value substituted in the equation ranged from 0 to 1.0. The results of this analysis are presented in Table 5, and show that the optimum "K" value derived from all the data points for each of the data sets. (i.e., the "K" values with the highest correlations) were not the same as the "K" values derived from all the data points as shown in Table 4. This discrepancy shows that the "K" value derived using all the data points is largely unreliable for achieving the highest correlation between the field spectra and the non-Lambertian model. Using all the data points for each of the solar elevations, it was found that "K" values from .5 to 1.0 would give correlation coefficients of greater than .90. The non-Lambertian model is relatively insensitive to variations in the empirical "K" value as derived by Smith et al (1979) (i.e., using all the data points regardless of aspect).

A second study was undertaken to examine the sensitivity of the model to variations in "K" for each of the aspect strings. The term "aspect string" is used to describe a series of radiance measurements taken for different slopes at one aspect. The correlation coefficients between the field spectra and the non-Lambertian model, substituting "K" values between 0 and 1.0 are presented in Table 6 (a, b, c, d). The model was most sensitive to the "K" value at those aspects near to solar azimuth. These aspect strings had the greatest range in radiance values. The "K" values which gave insignificant correlations with the field spectra were those which produced little change in the non-Lambertian value with change in radiance and occurred at the transition point between a negative and positive relationship. A "K" value of 1.0, i.e., the Lambertian model, would provide correlation coefficients of greater than 0.80 for all aspect strings and all data sets (Table 6 (a, b, c, d)). All but four cases examined with a "K" of 1.0 had correlation coefficients of greater than 0.95.

The final stage of the analysis was to apply the models to the field measured radiance data to examine their effectiveness at removing the topographic effect. The method adopted for applying the models was to multiply the radiance values by their respective normalization transformations derived from the two models. The aspect "K" values were used to derive the non-Lambertian transformations. This analysis was undertaken only on the red radiance data. Theoretically, the normalized radiances are equivalent to the radiances from a flat surface with the sun directly overhead ($\text{vis: } i = e = 0$). The resulting normalized values for each slope and aspect are presented in Table 7 (a, b, c, d). The range in the normalized values for each aspect indicates the effectiveness of the models in eliminating the topographic effect. The topographic effect has been completely removed if the range in radiance values is zero. Examination of the normalized radiance values for each aspect shows that in all cases the non-Lambertian model produced the optimum reduction in the topographic effect, confirming the results of the correlation analysis. Comparison of the range in radiance values associated with each aspect for the non-Lambertian model and the field measured radiance (Table 7 (a, b, c, d)) shows that in only one case the non-Lambertian model failed to reduce the topographic effect. This occurred at a 90 degree aspect where the smallest topographic effect in the data was observed. For all the aspects with a high range in field measured radiance, the non-Lambertian model substantially

reduced the topographic effect. The remaining variations in the normalized radiance for each aspect and the difference between the data sets may be due in part to the exclusion of any consideration of diffuse light in the model, in particular skylight and the light reflected from the surrounding ground surface. Kimes et al (1979) express the importance of including consideration of anisotropic sky irradiance in surface radiance models. The contribution of the diffuse light component to the topographic effect could not be determined from the data collected in this study but will be the subject of a further field experiment by the authors.

Summary of Results

The non-Lambertian model produced the overall highest statistical correlations with the field spectra, although consideration of exitance angle, implicit in the model, was shown to be less important for aspects away from solar azimuth, e.g., 90° . In these cases, the Lambertian model also yielded high correlations with the field spectra. The results of the analysis demonstrated that the Lambertian model was less suitable for simulating the spectral response at high solar elevations.

When the two models were applied to normalize the field measured data, the non-Lambertian model was found to be consistently superior to the Lambertian model at reducing the "topographic effect," confirming the results of the correlation analysis. The remaining variation in the normalized radiance values were thought to be largely due to a diffuse light component which was not addressed by the present model.

Detailed examination of the empirical constant "K" revealed that "K" was not a constant value for cover types varying only as a function of phase angle and wavelength but varied considerably with surface geometry, i.e., slope and aspect. The non-Lambertian model as used by Smith et al (1979) was improved by deriving the empirical value "K" for each aspect. The "K" values generally decreased with aspect, away from solar azimuth. The non-Lambertian model was more sensitive to variations in the "K" value at those aspects near to solar azimuth.

Potential Application of the Models to Remotely Sensed Data

The intention of the study was to examine the radiance simulation models for possible application to eliminating the topographic effect on Landsat data. As both the models reduce the radiance values to represent radiances from a flat surface with the sun directly overhead, they also have a potential application for reducing sun angle differences between multitemporal data sets. For application to Landsat data, both models require information concerning surface geometry. Such data is available for the United States in the form of digital terrain data provided by the USGS. Registration of the digital terrain data to the Landsat data and calculation of slope and aspect have been demonstrated by several studies (Stow and Estes, 1979; Strahler et al, 1978; and others). Digital elevation data with an improved resolution of 30m ground spacing are being made available in the form of Digital Elevation Model (DEM) Tapes by the Digital Application Group at USGS Reston (McEwen and Elassal, 1978).

The Lambertian model requires only slope and aspect data for any given Landsat pixel but as shown in this study is only effective for a restricted range of slopes and aspects. The non-Lambertian model is effective over a wider range of slopes and aspects but requires radiance information for specific cover types to calculate the empirical "K" value. Calculating "K" values for each cover type and each aspect is not a practical procedure and the authors suggest the following alternative possibilities, which will be the subject of a future study. Sytinskaya (1943) showed that "K" values for vegetated surfaces were substantially lower than for non-vegetated surfaces. It may be that a two or three level stratification of the Landsat data, based on a ratioed radiance transformation such as the normalized difference (Deering, et al., 1975 and Tucker, 1979) could be used to derive "K" values which would provide an improvement over the Lambertian model. Also, it may be possible to use the non-Lambertian model only for those aspects where the Lambertian model is ineffective and where the non-Lambertian model is sensitive to "K".

As a result of this study the authors believe there to be three main areas that require further research: first, the contribution of diffuse light to the "topographic effect" from both skylight and terrain scattering; second, examination of the application of the models to normalizing multi-temporal

data, specifically to examine the cause of the differences between the normalized radiance values at different solar elevations; third, the application of the models to Landsat data, using surface geometry derived from digital terrain data.

Bibliography

- Cicone, R. C., W. A. Malila, and E. P. Crist, 1977. Investigation of techniques for inventorying forested regions. Final Report: Vol. II Forestry information system requirements and joint use of remotely sensed and ancillary data. NAS-CR-ERIM 122700-35-F2, 146 pp.
- Deering, D. C., J. W. Rouse, R. H. Hass, and J. A. Schnell, 1975. Measuring forage production of grazing units from Landsat MSS data. Proc. of the Tenth International Symposium on Remote Sensing of Environment, Ann Arbor, Michigan, pp 1169-1178.
- Hoffer, R. M. and Staff, 1975. Computer analysis of Skylab multispectral scanner data in mountainous terrain for land use, forestry, water resource and geologic applications. LARS Information Note 1212275, 380 pp.
- Holben, B. N. and C. O. Justice, 1979. Evaluation and modeling of the topographic effect on the spectral response from nadir pointing sensors. NASA/GSFC T.M. 80305, 19 pp.
- Justice, C. O., 1978. An examination of the relationship between selected ground properties and Landsat MSS data in an area of complex terrain in southern Italy. Proc. American Society of Photogrammetry, Fall Meeting, Albuquerque, New Mexico, pp. 303-328.
- Kimes, D., J. A. Smith and K. J. Ranson, 1979. Interpreting vegetation reflectance measurements as a function of solar zenith angle. NASA/GSFC T.M. 80320, 29 pp.
- Kriebel, K. T., 1978. Measured spectral bi-directional reflection properties for four vegetated surfaces, Applied Optics, 9(6):1474-1475.
- McEwen, R. B. and A. A. Elssal, 1978. USGS Digital Cartographic Data Acquisition. Paper presented at the International Users Conference on Computer Mapping Hardware, Software and Data Bases. Harvard University: June 1978, 23 pp.

- Minnaert, M., 1941. The reciprocity principle in lunar photometry. *Journal of Astrophysics* 93: 403-410.
- Minnaert, M., 1961. Photometry of the Moon. in G. P. Kuiper (ed.) *The Solar System Vol. III. Planets & Satellites*. University of Chicago Press, pp 213-249.
- Monteith, J. L., 1973. *Principles of Environmental Physics*. Edward Arnold: 241 pp.
- Sadowski, F. G. and W. A. Malila, 1977. Investigation of techniques for inventorying forested regions: Vol. 1: Reflectance modeling & empirical multispectral analysis of forest canopy components. NAS-CR-ERIM-122700-35-F1.
- Smith, J. A., Tseu Lie Lin and K. J. Ranson, 1979. The Lambertian assumption and Landsat data. Paper accepted for publishing by Photogrammetric Engineering and Remote Sensing.
- Stow, D. A. and J. E. Estes, 1979. Analyzing accuracy attributes of Landsat and digital terrain tape data in the context of digital geobase information system. *Proc. of the Symposium on Machine Processing of Remotely Sensed Data*. LARS Purdue, pp. 193-200.
- Strahler, A. H., T. L. Logan, and N. A. Bryant, 1978. Improving cover classification accuracy from Landsat by incorporating topographic information. *Proc. of the International Symposium on Remote Sensing of the Environment*. Ann Arbor, Michigan, Vol. 2:pp. 927-956.
- Sytinskaya, N. N., 1949. Determination of the degree of smoothness of planets by photometric methods. *Uchenye Zapiski, L. G. U. No. 116. (59-311-41:Translated 1959)* – NASA NG3-81360, 18 pp.
- Tucker, C. J., 1979. Red and photographic infrared linear combinations for monitoring vegetation. *Remote Sensing of the Environment* 8:127-150.

Acknowledgment

The authors thank Jim Tucker, Dan Kimes and Maryann Karinch.

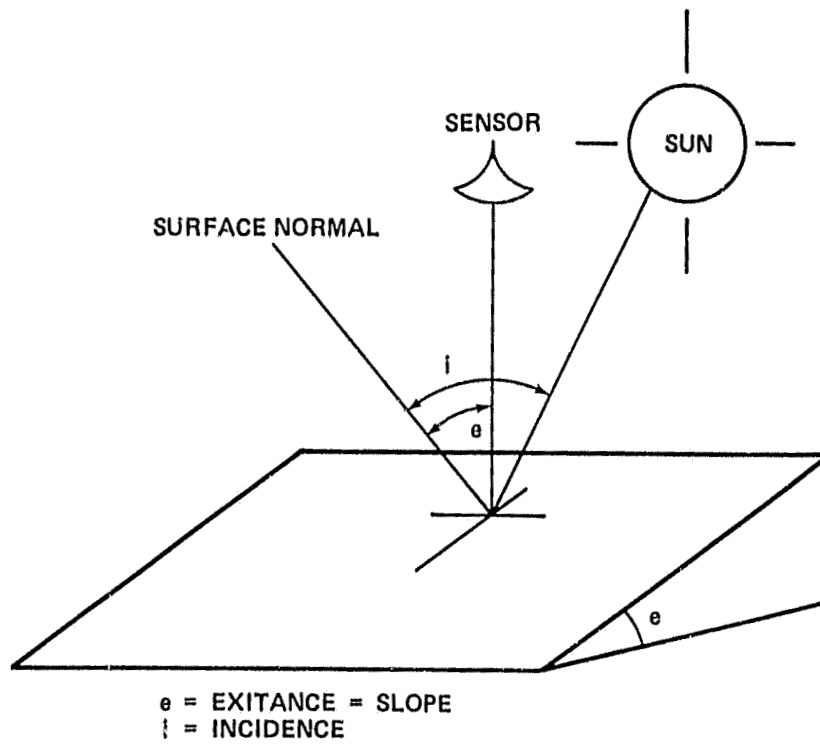


Figure 1. Angles used in the radiance models

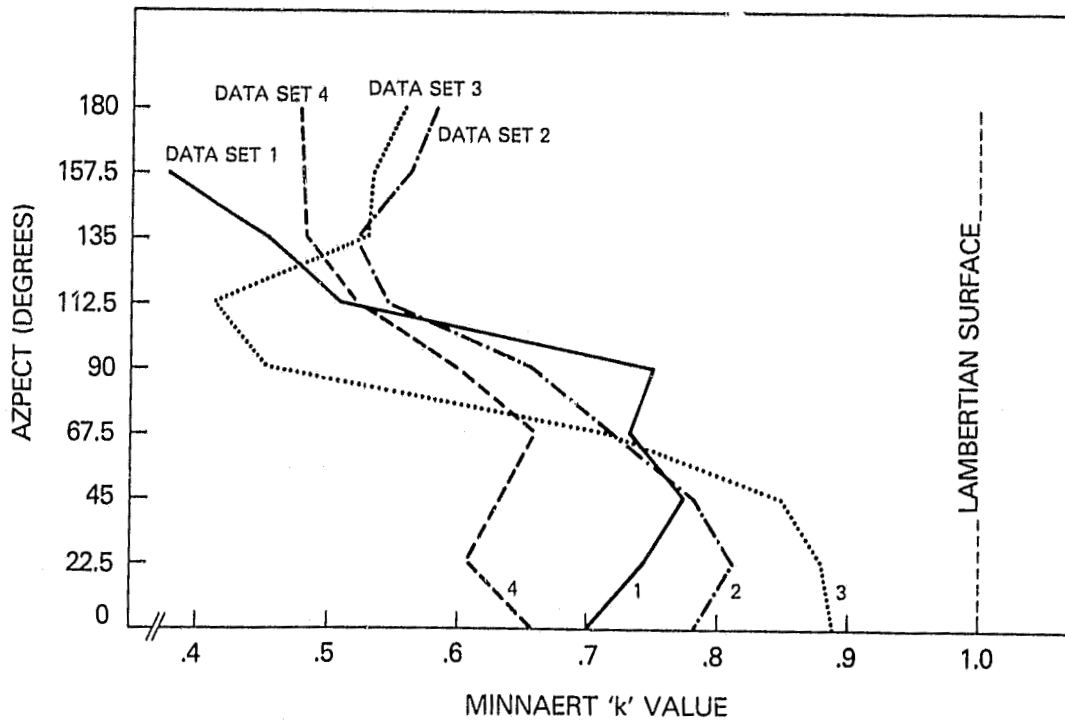


Figure 2. Minnaert 'K' values plotted against aspect for four data sets

Table 1
Table to show the Minnaert 'K' value for the four hand-held radiometric data sets using all data points.

Data Set	1	2	3	4
Solar Elevation	14°	35°	40°	61°
Phase Angle	76°	55°	50°	29°
Minnaert Constant 'K'	.663	.578	.504	.513

Table 2
Table to show the Minnaert 'K' value calculated for each aspect of the four hand-held radiometric data sets.

Data Sets	1	2	3	4
Phase Angle	76°	55°	50°	29°
Aspect (in degrees)	(K values)			
0	.701	.893	.783	.661
22	.744	.884	.812	.608
45	.774	.849	.780	.633
67.5	.734	.723	.719	.660
90	.751	.658	.451	.600
112.5	.509	.548	.413	.552
135	N/D	.524	.531	.483
157.5	N/D	.564	.513	N/D
180	N/D	.584	.563	N/D

N/D = insufficient data available

Table 3
Table to show the Minnaert 'K' value calculated for each slope strata
of the four hand-held radiometric data sets.

Data Set	1	2	3	4
Slope (in degrees)				
10	.391	.665	.774	.612
20	.442	.667	.660	.548
30	.691	.603	.574	.550
40	.673	.575	.485	.534
50	.626	.583	.514	.505
60	.604	.509	.414	.409
70	.586	.519	.474	.345

Table 4
Correlation Coefficients (r) between radiance field measurements and two simulation models
for each aspect for four solar elevations. "L" and "NL" represent Lambertian and
non-Lambertian models, respectively.

Aspect (in degrees)	Solar Elevation 14°		Solar Elevation 35°		Solar Elevation 40°		Solar Elevation 61°	
	L	NL	L	NL	L	NL	L	NL
	0	.932	.928	.960	.962	.896	.955	X
22.5	.979	.997	.982	.994	.944	.999	X	.997
45.	.985	.998	.956	.993	.805	.995	X	.983
67.5	.936	.996	X	.980	X	.980	.775	.918
90.	.980	.990	.965	.983	.992	.990	.937	.969
112.5	.997	.983	.996	.998	.975	.997	.929	.971
135.	N/D		.995	.997	.992	1.000	.982	1.000
157.5	N/D		.998	.998	.994	.980	N/D	
180.	N/D		.996	.990	.999	.992	N/D	
All Pts.	.961	.963	.959	.954	.929	.934	.909	.962

N/D = insufficient data. X = insignificant at the .05 level.

9-26-78 9-5-78 9-25-78 8-24-78

Table 5
 Table to show correlation (r values) of the non-Lambertian model to the field measured radiances,
 substituting k values from 0 to 1.0

k values	Data Set 1 n = 112		Data Set 2 n = 117		Data Set 3 n = 104		Data Set 4 n = 64	
	Red	IR	Red	IR	Red	IR	Red	IR
0	.256	.267	.231	.292	.569	.590	-.418	-.366
0.1	.433	.446	.469	.519	.711	.731	-.224	-.174
0.2	.605	.619	.624	.667	.812	.831	.085	.129
0.3	.751	.764	.761	.793	.879	.896	.490	.521
0.4	.856	.868	.865	.888	.920	.936	.813	.827
0.5	.924	.934	.932	.944	.944	.960	.954	.955
0.6	.960	.968	.965	.968	.958	.973	.986	.979
0.7	.975	.982	.973	.969	.965	.979	.979	.967
0.8	.977	.982	.965	.954	.967	.980	.956	.945
0.9	.971	.974	.947	.932	.965	.978	.933	.920
1.0	.959	.961	.929	.909	.961	.976	.908	.900

Table 6
(a, b, c, d) show the correlation (r) values between field measured red radiance
and the non-Lambertian models substituting K values from 0 to 1.0.

Table 6(a) Data Set (9/26/78) Solar Elevation = 11°

Aspect (in degrees)	K value										
	0	.1	.2	.3	.4	.5	.6	.7	.8	.9	1.0
0	.76	.80	.83	.86	.88	.90	.92	.93	.83	.93	.93
45	.84	.87	.89	.92	.95	.97	.98	.99	1.0	1.0	1.0
90	-.99	-.99	-.99	-.99	-.99	-.96	.99	.99	.99	.98	.98
135						N/A					
180						N/A					
225						N/A					
270	.82	.83	.84	.85	.86	X	-.88	-.88	-.89	-.89	-.90
315	.80	.84	.87	.90	.93	.95	.97	.99	1.0	1.0	1.0

N/A = no data available

X = insignificant at the 0.05 level

Table 6(b) Data Set (9/05/78) Solar Elevation = 35°

Aspect (in degrees)	K value										
	0	.1	.2	.3	.4	.5	.6	.7	.8	.9	1.0
0	.64	.68	.71	.75	.80	.84	.88	.92	.95	.96	.96
45	X	.70	.73	.77	.81	.85	.90	.95	.98	.99	.96
90	-.99	-.99	-.99	-.99	-.99	X	.98	.98	.98	.97	.96
135	-.98	X	.97	.98	.99	1.0	1.0	1.0	1.0	1.0	1.0
180	-.96	.95	.97	.98	.98	.99	.99	.99	.99	.99	1.0
225	-.97	-.96	.96	-.98	.98	.99	.99	1.0	1.0	1.0	1.0
270	-.96	-.95	-.95	-.94	-.94	X	.92	.91	.90	.89	.88
315	.82	.84	.86	.89	.92	.95	.97	.99	1.0	.96	.87

X = insignificant at the 0.05 level

Table 6(c) Data Set (9/25/78) Solar Elevation = 40°

Azpect (in degrees)	K value										
	0	.1	.2	.3	.4	.5	.6	.7	.8	.9	1.0
0	.72	.75	.79	.81	.85	.89	.92	.95	.96	.94	.90
45	.76	.78	.80	.83	.88	.90	.94	.98	.99	.95	.80
90	-.96	-.97	-.98	-.98	-.99	X	.99	.99	.99	.99	.99
135	-.98	-.97	-.99	1.0	1.0	1.0	1.0	1.0	1.0	.99	.99
180	-.95	X	.99	.99	.99	.99	.99	.99	1.0	1.0	1.0
225	-.98	-.97	.97	.99	1.0	1.0	1.0	1.0	1.0	1.0	1.0
270	-.97	-.98	-.98	X	X	X	.99	.99	.99	.98	.98
315	.81	.83	.85	.87	.90	.93	.96	.97	.92	X	X

X = insignificant at the 0.05 level

Table 6(d) Data Set (8/24/78) Solar Elevation = 61°

Azpect (in degrees)	K value										
	0	.1	.2	.3	.4	.5	.6	.7	.8	.9	1.0
0	.87	.89	.90	.92	.94	.97	.99	.99	.95	.81	X
45	.78	.80	.82	.84	.87	.91	.97	.92	X	X	X
90	-.99	-.99	-.98	-.98	-.98	X	.97	.96	.95	.95	.94
135	-.98	-.99	-.98	X	.99	1.0	1.0	.99	.99	.99	.98
180	-.97	-.98	X	.90	.96	.98	.99	1.0	1.0	1.0	.99

X = insignificant at the 0.05 level.

Table 7(a)

Table to show the results of applying the two radiance models to the red radiance field spectra

Data Set: 9-26-78												
Sun Elevation (degrees):		11		14		14		14		13		
Azpect (degrees):		0		22.5		45		67.5		90		
Model:		L	NL	L	NL	L	NL	L	NL	L	NL	
Slope:		0	96.9	58.6	103.8	72.8	102.6	74.6	101.3	69.1	100.0	69.3
		10	76.4	55.7	89.6	70.6	86.5	68.4	87.4	63.1	97.1	66.8
		20	72.5	58.2	83.3	70.0	86.3	71.5	88.5	65.9	101.6	68.4
		30	69.0	58.2	79.8	69.2	84.9	71.9	89.6	67.1	105.3	68.0
		40	69.8	59.7	72.7	65.5	86.1	73.0	90.2	66.8	113.0	68.6
		50	69.9	58.8	80.4	68.8	86.5	71.8	93.8	66.9	127.1	70.9
		60	72.0	57.5	84.5	68.8	89.4	70.9	100.0	66.8	145.7	71.8
Range:			24.9	4.0	23.4	7.3	17.7	6.2	13.9	6.0	48.6	5.0
Red Radiance Range:			53		50		39		20		6	
Sun Elevation (degrees):		13		12		12		12				
Azpect (degrees):		112.5		135		157.5		180				
Model:		L	NL	L	NL	L	NL	L	NL			
Slope:		0	103.8	49.5	102.4	47.5	101.0	46.0	102.7	46.4		
		10	117.6	46.4	165.5	49.4	254.7	54.9	254.6	44.8		
		20	174.5	49.0								
		30										
		40										
		50										
		60										
Range:			71	3.1	63.1	1.9	153.7	8.9	151.9	2.4		
Red Radiance Range:			16		15		14		15			

Table 7(b)

Data Set: 9-25-78											
Sun Elevation (degrees):		35		35		36		37			
Aspect (degrees):		0		22.5		45		67.5			
Model:		N	NL	N	NL	N	NL	N	NL		
Slope:	0	109.2	94.1	105.0	94.8	110.3	98.1	108.5	93.9		
	10	103.9	94.3	101.1	94.3	103.0	94.3	105.8	93.0		
	20	99.3	92.7	99.6	94.5	102.8	95.1	105.0	92.1		
	30	98.5	92.8	100.1	95.1	104.2	96.0	107.1	92.0		
	40	99.1	91.7	102.3	95.9	107.4	96.9	114.3	94.2		
	50	102.3	91.4	104.3	95.0	112.7	97.8	119.4	92.9		
	60	107.5	89.5	118.1	95.8	119.1	97.1	134.5	94.3		
Range:		10.7	4.8	18.5	1.5	16.3	3.8	29.5	2.3		
Red Radiance Range:		45		43		29		11			
Sun Elevation (degrees):		37		38		39		39		40	
Aspect (degrees):		90		112.5		135		15.5		180	
Model:		N	NL	N	NL	N	NL	N	NL	N	NL
Slope:	0	109.2	81.3	105.5	79.4	105.3	84.6	108.7	83.2	110.4	91.0
	10	109.3	79.9	112.0	78.5	114.5	84.0	115.6	76.4	120.0	88.0
	20	112.7	78.0	124.4	77.4	134.9	85.3	130.7	68.2	137.4	83.7
	30	122.1	76.9	144.3	75.3	168.4	84.8	197.4	69.0	207.3	90.6
	40	133.8	73.0	180.3	72.6	251.8	84.4				
	50	151.6	67.4	260.5	67.8						
	60	181.9	60.2	749.4	81.2						
Range:		72.7	21.1	148.5	11.4	146.5	1.3	88.7	15.0	96.9	7.3
Red Radiance Range:		11		31		50		54		57	

Table 7(c)

Data Set: 8-24-78												
Sun Elevation (degrees):		62		62		62		62		62		
Aspect (degrees):		0		22.5		45		67.5		90		
Model:		N	NL	N	NL	N	NL	N	NL	N	NL	
Slope:		0	91.1	87.2	89.7	85.3	93.0	88.8	92.9	89.0	91.6	87.1
		10	90.7	88.6	88.0	85.5	90.7	87.7	91.0	87.4	91.8	86.4
		20	91.0	88.8	88.0	85.1	92.2	88.2	94.3	88.7	96.3	87.2
		30	92.0	87.6	91.7	86.0	96.7	89.4	98.3	88.7	105.7	89.7
		40	96.9	89.9	97.3	86.1	103.3	89.5	106.0	89.5	118.0	90.8
		50	105.3	88.4	105.4	85.1	113.1	88.0	119.2	91.1	133.5	89.3
		60					127.4	88.0	133.9	87.8	162.5	88.9
Range:			14.2	1.6	17.4	1.0	22.4	1.5	12.8	3.7	71.9	4.4
Red Radiance Range:			18		16		11		4		9	
Data Set: 8-24-78												
Sun Elevation (degrees):		62		62		62		62		62		
Aspect (degrees):		112.5		135		157.5		180		180		
Model:		N	NL	N	NL	N	NL	N	NL	N	NL	
Slope:		00	88.1	83.4	93.7	88.0	90.3	85.0	93.7	88.2		
		10	92.8	85.3	95.7	85.4	96.5	85.6	94.7	83.7		
		20	101.2	87.6	105.6	86.2	104.9	84.3	105.4	83.9		
		30	113.7	89.5	121.0	86.5	119.6	82.7	117.9	80.2		
		40	133.1	91.3	147.9	86.9	144.3	80.0	144.9	78.1		
		50	162.0	91.3	195.4	86.0	204.0	80.1	206.5	76.4		
		60	218.0	91.6	322.5	86.8						
Range:			129.9	8.2	228.8	2.0	113.7	5.5	112.8	11.8		
Red Radiance Range:			15		32		45		56			

Table 7(d)

Data Set: 9-05-78												
Sun Elevation (degrees):		29		30		31		32		33		
Azpect (degrees):		0		22.5		45		67.5		90		
Model:		L	NL	L	NL	L	NL	L	NL	L	NL	
Slope:		0	91.0	84.0	90.9	84.0	90.7	82.1	90.8	76.1	89.1	72.1
		10	89.2	84.7	84.7	80.3	87.9	81.5	88.5	75.6	92.2	73.9
		20	86.2	83.1	82.9	79.5	88.0	82.5	88.9	76.1	95.8	75;1
		30	82.9	80.3	82.5	79.4	89.3	83.7	90.3	76.0	102.9	75.5
		40	84.7	81.7	84.4	80.8	91.7	84.9	94.6	76.7	113.8	76.8
		50	82.5	78.6	87.6	82.6	94.1	85.1	103.5	79.1	126.8	75.9
		60	87.0	80.8	90.1	82.6	99.7	86.5	111.7	78.0	148.7	74.9
Range:			3.5	4.4	8.4	4.6	11.8	5.0	21.4	3.5	59.6	4.7
Red Radiance Range:			43		39		31		13		9	
Sun Elevation (degrees):		33		34		35						
Azpect (degrees):		112.5		135		157.5		180				
Model:		N	NL	N	NL	N	NL	N	NL			
Slope:		0	94.5	72.1	95.0	71.9	95.1	75.3	93.2	74.3		
		10	98.7	71.0	105.0	71.1	107.6	73.8	107.2	74.9		
		20	110.6	71.6	120.4	68.3	127.7	70.7	116.7	65.3		
		30	126.7	70.5	158.6	67.0	206.3	74.4	212.5	74.9		
		40	157.1	69.7	335.9	71.5						
		50	240.7	72.1								
		60										
Range:			146.2	2.4	240.9	4.9	111.3	3.7	119.3	9.4		
Red Radiance Range:			26		36		31		34			

BIBLIOGRAPHIC DATA SHEET

1. Report No.	2. Government Accession No.	3. Recipient's Catalog No.	
4. Title and Subtitle		5. Report Date	
		6. Performing Organization Code Code 923	
7. Author(s) Chris Justice Brent Holben		8. Performing Organization Report No.	
9. Performing Organization Name and Address Earth Resources Branch, Code 923 Goddard Space Flight Center Greenbelt, Maryland 20771		10. Work Unit No.	
		11. Contract or Grant No.	
		13. Type of Report and Period Covered	
12. Sponsoring Agency Name and Address NASA/Goddard Space Flight Center Greenbelt, Maryland 20771		14. Sponsoring Agency Code	
		15. Supplementary Notes	
16. Abstract			
<p>The differential illumination of surfaces due to slope angle and aspect variations produces a phenomenon known as the "topographic effect". This effect complicates the task of multi-spectral cover classification using remotely sensed satellite data of mountainous terrain. As a preliminary step to developing a technique to eliminate the topographic effect from remotely sensed data, two radiance simulation models were examined and compared. A Lambertian and a non-Lambertian model were tested using hand-held radiometer measurements from a uniform surface at different slope angle aspect orientations. A two-band, hand-held radiometer, filtered for the red and photographic infrared portion of the spectrum, was used to measure the radiance from a uniform sand surface over a range of solar elevations.</p> <p>Linear correlation coefficients for the non-Lambertian model and the field spectra were calculated to be greater than 0.92 for all cases; whereas correlation coefficients for the Lambertian model ranged from 0.06 to 0.98. An assumption regarding an empirical constant within the non-Lambertian equation was found to be invalid and the model was improved by using subsets of the data to derive the empirical value.</p>			
17. Key Words (Selected by Author(s)) Radiance Modeling, Remote Sensing, Lambertian, Non-Lambertian, Topographic Effect		18. Distribution Statement	
19. Security Classif. (of this report) Unclassified	20. Security Classif. (of this page) Unclassified	21. No. of Pages	22. Price*